DOI: 10.1111/cgf.12427
Eurographics Symposium on Geometry Processing 2014
Thomas Funkhouser and Shi-Min Hu
(Guest Editors)

Volume 33 (2014), Number 5

Discrete 2-Tensor Fields on Triangulations

Fernando de Goes[1] Beibei Liu[2] Max Budninskiy[1] Yiying Tong[2] Mathieu Desbrun[1,3]

[1]Caltech [2]MSU [3]INRIA Sophia-Antipolis Méditerranée

Abstract

Geometry processing has made ample use of discrete representations of tangent vector fields and antisymmetric tensors (i.e., forms) on triangulations. Symmetric 2-tensors, while crucial in the definition of inner products and elliptic operators, have received only limited attention. They are often discretized by first defining a coordinate system per vertex, edge or face, then storing their components in this frame field. In this paper, we introduce a representation of arbitrary 2-tensor fields on triangle meshes. We leverage a coordinate-free decomposition of continuous 2-tensors in the plane to construct a finite-dimensional encoding of tensor fields through scalar values on oriented simplices of a manifold triangulation. We also provide closed-form expressions of pairing, inner product, and trace for this discrete representation of tensor fields, and formulate a discrete covariant derivative and a discrete Lie bracket. Our approach extends discrete/finite-element exterior calculus, recovers familiar operators such as the weighted Laplacian operator, and defines discrete notions of divergence-free, curl-free, and traceless tensors—thus offering a numerical framework for discrete tensor calculus on triangulations. We finally demonstrate the robustness and accuracy of our operators on analytical examples, before applying them to the computation of anisotropic geodesic distances on discrete surfaces.

Categories and Subject Descriptors (according to ACM CCS): Computer Graphics [I.3.5]: Computational Geometry and Object Modeling—Curve and surface representations.

1 Introduction

While scalar (rank-0 tensor) and vector (rank-1 tensor) fields have been staples of geometry processing, the use of rank-2 tensor fields has steadily grown over the last decade in applications ranging from non-photorealistic rendering to anisotropic meshing. Unlike their lower rank counterparts, there is currently no convenient way to perform computations with arbitrary 2-tensor fields on triangulations. In this paper, we present a coordinate-free representation of rank-2 tensors suitable for tensor calculus on triangle meshes. Derived from an orthogonal decomposition of planar 2-tensor fields, our resulting discrete tensors extend the notion of discrete differential forms, and are thus compatible with discrete or finite-element exterior calculus in that they define pairing and inner products of arbitrary forms. Additionally, pervasive discrete geometry processing tools such as the weighted Laplace-Beltrami operator are shown to be special cases of our construction, while new operators such as the covariant derivative of discrete 1-forms emerge.

1.1 Related Work

In order to put our contributions in perspective, we review representative topics that our work impacts or extends.

Tangent Vectors. Vector fields on triangulations are often discretized through local coordinates related to orthogonal frames defined either on vertices or on faces. A continuous vector field over a mesh is evaluated from this finite set of vectors based on piecewise constant interpolation [PP00] or, to increase smoothness, using non-linear basis functions derived from the geodesic polar map [ZMT06, KCPS13]. In an effort to remove the need for coordinate systems, scalar potentials were proposed as an intrinsic encoding of tangent vector fields: while Tong et al. [TLHD03] used two potential values per node interpolated with linear finite elements, Polthier and Preuss [PP03] offered a discrete notion of Hodge decomposition with proper cohomology by using one value per node and one value per unoriented edge interpolated with conforming and non-conforming linear basis functions respectively. This representation is, however, limiting as it only leads to per-face constant vector fields. Operator-based representations have also been recently proposed [PMT*11, ABCCO13], but their use is, to date, too restrictive to be widely adopted. Finally, a coordinate free approach to vector field representation was introduced through the use of algebraic topology and exterior calculus [FSDH07] where vector fields are identified as discrete differential 1-forms (i.e., rank-1 tensors of type $(0,1)$) and interpolation is performed via Whitney basis functions [Whi57]. These edge-based discrete tangent vector fields have since then been shown useful in a variety of ap-

plications [ETK*07, BCBSG10]. Our discrete 2-tensor fields will be fully compatible with this specific form-based representation, and will even provide a discrete notion of covariant derivative of vector and covector fields.

2-Tensors. Tensors of rank two are commonplace in geometry processing, e.g., as a way to encode sizing and orientation fields for meshing purposes [FH96, NSO12, PPTSH14]. These mathematical objects can act on tangent vector fields, on 1-forms, or on both (i.e., tensors of type $(0,2)$, $(2,0)$, and $(1,1)$ respectively). Much like early work on discrete vector fields, they are often defined by first establishing a local tangent space basis per vertex [NSO12], edge [ACSD*03], or face [TSS*04, ZRS05, IO06], then storing the four components of the tensor in each of these frames. A notable coordinate-free alternative exists for purely *antisymmetric* 2-tensors (called 2-forms): they are scalar multiples of $J = \left(\begin{smallmatrix} 0 & -1 \\ 1 & 0 \end{smallmatrix}\right)$ in any orthogonal coordinate frame since $RJR^t = J$ for an arbitrary rotation matrix R. They can thus be encoded as discrete differential 2-forms via one scalar per face and Whitney basis functions [AFW06b, DKT08]. (Dual 2-forms, defined per dual cell, can also be used.) In comparison, symmetric tensors have rarely been discussed in the discrete realm [Mei03, KASH13], yet they are implicitly behind all inner products of forms or vectors, generalized Laplacian operators [AN02], and the notion of Hodge star [BH06]. Our discrete encoding of tensors encompasses both symmetric and antisymmetric tensors in a consistent framework.

Analysis and Visualization. Visualization of fluid motion is often achieved by analyzing the gradient of the velocity field [LW09]. This 2-tensor field is often split into an antisymmetric part conveying vorticity, and a symmetric part that can be depicted via streamlines tangent to tensor eigenvectors [DH94]. A unified analysis of arbitrary 2-tensors was proposed in [ZP05] based on complex eigenvalues and eigenvectors. Zhang et al. [ZYLL09] used, instead, a geometric decomposition of 2-tensors leveraging the trace operator, which was later illustrated as a combination of streamlines and glyphs [PLC*11]. In contrast, our work introduces a new orthogonal decomposition of planar 2-tensor fields compatible with discrete exterior calculus.

Metrics. The metric tensor of a Riemannian surface is, itself, a symmetric tensor that defines the length of, and angle between, tangent vectors. While most geometry processing methods use the canonical metric of a mesh induced by its Euclidean embedding, one can use a set of edge lengths to encode piecewise-Euclidean metrics [Reg61, SSP08, Luo10]. However, high degrees of anisotropy might not be representable with pure edge lengths as they might not fulfill the triangle inequality everywhere [KMZ11, CHK13]. Recently, a notion of discrete divergence-free metric tensor in the plane was introduced in [dGAOD13] (representing stress tensors within masonry structures) through not only edge lengths but also additive weights per vertex—which affect both the discrete Hodge star and the Laplacian operator. This augmented metric was further extended to surface meshes in [dGMMD14]. Our approach offers a generalization of this divergence-free case to arbitrary rank-2 tensors.

Elasticity. Decompositions of differential 2-tensors such as stress and strain are particularly relevant in elasticity [Hu54]. Arnold et al. [AFW06a] proposed tensor subspaces (including divergence-free tensors) that form an exact chain dubbed the *elasticity complex*. This sequence further served as the basis for discretizing planar symmetric 2-tensor (stress) fields through mixed finite elements [AW02] or non-conforming elements [AW03]. Extensions to tetrahedral meshes were proposed in [AAW08, AAW14]. Also in the elasticity context, Kanso et al. [KAT*07] expressed 2-tensor fields as quadratic tensor products of Whitney 1-forms. While previous methods require high order finite-element spaces, we discretize arbitrary 2-tensor fields through direct differentiation of piecewise-linear Whitney basis functions, which leads to closed-form expressions for discrete tensor calculus on triangulations.

1.2 Contributions

We introduce a numerical framework to encode and manipulate rank-2 tensors on triangle meshes. Our work is based on a novel coordinate-free decomposition of continuous 2-tensor fields in the plane. By leveraging this decomposition, we construct a finite-dimensional representation of 2-tensors on discrete surfaces that is fully compatible with the DEC [DKT08] and FEEC [AFW06b] machinery. Our discrete 2-tensors exactly mimic the continuous notion of divergence-free, curl-free, and traceless tensors, and recover many well-known discrete operators commonly used in geometry processing. Finally, our approach offers a discrete counterpart to both covariant derivative and Lie bracket of 1-forms (or vector fields), and provides an extension of the heat method [CWW13] to compute anisotropic geodesics.

1.3 Notations

We will make use of a few specific notations in this paper.

Continuous setup. We denote by $\mathcal{M}$ a smooth and compact Riemannian 2-manifold, possibly with boundaries $\partial\mathcal{M}$, and endowed with a metric $\mathfrak{g}$ that provides an inner product on (tangent) vector fields. We also use the notion of k-forms ($k = 0, 1, 2$), along with their respective inner products $\langle .,. \rangle_k$, and the operators d and $\star$ on these forms [AMR88]. We denote by Δ the Laplace-Beltrami operator on functions. From the metric, one can convert a vector field $\mathbf{v}$ into an equivalent 1-form ω using the flat ($\flat$) operator, i.e., $\mathbf{v}^\flat = \omega$; similarly, a 1-form is converted into its equivalent vector field by the sharp ($\sharp$) operator, i.e., $\omega^\sharp = \mathbf{v}$. We call $\mathcal{T}$ the space of tensor fields of rank $(0,2)$ on $\mathcal{M}$, i.e., 2-tensors acting on vector fields. We also define a local basis of tensors in a given coordinate frame as:

$$I = \left(\begin{smallmatrix} 1 & 0 \\ 0 & 1 \end{smallmatrix}\right), \quad J = \left(\begin{smallmatrix} 0 & -1 \\ 1 & 0 \end{smallmatrix}\right), \quad B = \left(\begin{smallmatrix} 0 & 1 \\ 1 & 0 \end{smallmatrix}\right), \quad C = \left(\begin{smallmatrix} 1 & 0 \\ 0 & -1 \end{smallmatrix}\right).$$

We write the area form of $\mathfrak{g}$ as $\mu_\mathfrak{g} = \sqrt{\det \mathfrak{g}}\, J^t$, and the Hodge star on 1-forms as $\star = \sqrt{\det \mathfrak{g}}\, J \mathfrak{g}^{-1}$, indicating a rotation by $\pi/2$ in the tangent plane when applied to a covector. Finally,

the (Frobenius) inner product on 2-tensor fields is:

$$\forall \tau_1, \tau_2 \in \mathcal{T}, \quad \langle \tau_1, \tau_2 \rangle_F = \int_{\mathcal{M}} \operatorname{tr}(\tau_1^t \, \mathfrak{g}^{-1} \tau_2) \, \mu_{\mathfrak{g}}, \qquad (1)$$

where $\operatorname{tr}(\tau) = \tau_{ij} \mathfrak{g}^{ij}$ indicates the trace operator on 2-tensors.

Discrete setup. When dealing with a discrete surface, we use an orientable, compact, and 2-manifold simplicial complex M in $\mathbb{R}^3$, of arbitrary topology (possibly with boundary ∂M). We call $\mathcal{V}$ the set of all its vertices, while the corresponding edge and face sets are denoted by $\mathcal{E}$ and $\mathcal{F}$. Each edge and triangle carries an arbitrary but fixed orientation (index order matters; e.g., ij has the opposite orientation as ji), while vertices have positive orientation by convention. Vertices are given positions $P = \{p_i \in \mathbb{R}^3\}$, which define the surface through linear interpolation over each simplex. The resulting Euclidean measures of edges and triangles are denoted by l_{ij} (length) and a_{ijk} (area), where the indices refer to the vertex indices, and we assume these to be all nonzero. We denote by θ_{ijk} the angle between edges ij and jk of a triangle ijk. Discrete k-forms are given as scalars on k-cells [DKT08]. Moreover, we indicate as $\mathbf{d}_0$ the transpose of the incidence matrix of vertices and edges ($|\mathcal{E}|$ rows, $|\mathcal{V}|$ columns), in which each row contains a single $+1$ and -1 for the endpoints of a given edge (the sign being determined from the chosen edge orientation), and zero otherwise; and by $\mathbf{d}_1$ the transpose of the incidence matrix of edges and faces ($|\mathcal{F}|$ rows, $|\mathcal{E}|$ columns), with $+1$ or -1 entries according to the orientation of edges as one moves counterclockwise around a face. We also use Whitney basis functions for discrete forms [Whi57], indicated as ϕ_i (the usual piecewise linear finite-element function with $\phi_i(p_i) = 1$, $\phi_i(p_j) = 0$) for 0-forms, $\phi_{ij} = \phi_i d\phi_j - \phi_j d\phi_i$ for 1-forms, and $\phi_{ijk} = 2 d\phi_i \wedge d\phi_j$ for 2-forms. By sharpening 1-form basis functions with the piecewise Euclidean metric, we get the corresponding basis functions for vector fields $\boldsymbol{\phi}_{ij} = \phi_{ij}^{\sharp} = \phi_i \nabla \phi_j - \phi_j \nabla \phi_i$. Hence, our discrete treatment will represent a vector field $\mathbf{u}$ and its associated 1-form $\alpha = \mathbf{u}^{\flat}$ through the same edge values α_{ij}, i.e., through $\mathbf{u} = \sum_{ij} \alpha_{ij} \boldsymbol{\phi}_{ij}$ and $\alpha = \sum_{ij} \alpha_{ij} \phi_{ij}$.

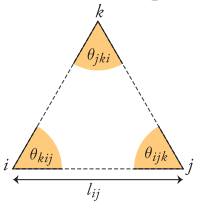

2 Tensor Fields over Smooth Surfaces

We begin with a brief review of existing decompositions of arbitrary rank-2 tensors on smooth surfaces $\mathcal{M}$ with boundaries $\partial\mathcal{M}$. Note that we will restrict our exposition to tensors of type $(0,2)$ (i.e., acting on tangent vectors), but equivalent expressions for tensors of type $(1,1)$ or $(2,0)$ can be derived using proper raising or lowering of indices with the flat and sharp operators defined by the Riemannian metric $\mathfrak{g}$.

2.1 Antisymmetric vs. Symmetric Tensors

Just as a matrix A can be decomposed into a symmetric $\frac{1}{2}(A + A^t)$ and an antisymmetric $\frac{1}{2}(A - A^t)$ part, a rank-2 tensor field $\tau \in \mathcal{T}$ can be decomposed into an antisymmetric (or skew-symmetric) tensor $\mu \in \mathcal{A}$ and a symmetric tensor $\sigma \in \mathcal{S}$ with $\tau = \mu + \sigma$. Therefore,

$$\mathcal{T} = \mathcal{A} \oplus \mathcal{S}. \qquad (2)$$

This decomposition is trivially an orthogonal direct sum for the Frobenius inner product $\langle .,. \rangle_F$ due to the fact that the product of an antisymmetric matrix and a symmetric matrix is traceless, and thus their inner product vanishes. Note that antisymmetric tensors are also called "forms", and have been extensively used as the basis of exterior calculus [AMR88]. Common geometric notions such as metric, stress, and strain are, instead, symmetric tensors.

2.2 Decomposition of Antisymmetric 2-Tensors

Antisymmetric rank-2 tensors $\mu \in \mathcal{A}$, dubbed 2-forms, are particularly simple on surfaces: they are of the form $\mu = s \, \mu_{\mathfrak{g}}$ where s is an arbitrary scalar function. They can be further decomposed, via Hodge decomposition [AMR88], as the orthogonal direct sum $\mu = d\omega \oplus h$, where ω is an arbitrary 1-form and h is a harmonic 2-form—which is simply a constant p times $\mu_{\mathfrak{g}}$ if $\mathcal{M}$ has a single connected component. Consequently, by applying the Hodge decomposition on ω, we see that 2-forms can be written in full generality as:

$$\mu = s \, \mu_{\mathfrak{g}} = (\Delta q + p) \, \mu_{\mathfrak{g}}, \qquad (3)$$

where Δq is the Laplacian of a scalar function q, and p is a scalar constant (non-zero constant functions are, indeed, not in the image of the Laplacian operator).

2.3 Decomposition of Symmetric 2-Tensors

Symmetric rank-2 tensors can also be decomposed further. Berger and Ebin [BE69] were the first to propose a notion of decomposition of symmetric tensors on *arbitrary* manifolds that extends the well-known Hodge decomposition of vector fields and forms. Noticing the role of the kernel and image of divergence and curl in the Hodge decomposition, they proposed to orthogonally decompose a symmetric tensor via the image of an operator P (with injective principal symbol) and the kernel of its adjoint operator P^* (uniquely defined via $\langle P \cdot, \cdot \rangle_F = \langle \cdot, P^* \cdot \rangle$ up to boundary conditions):

$$\mathcal{S} = \operatorname{Im} P \oplus \operatorname{Ker} P^*. \qquad (4)$$

This is the generalization of the well-known fact that, for any given matrix, its range and the kernel of its transpose form an orthogonal decomposition of the entire space. We review relevant examples of this versatile construction next.

Divergence-based expression. One of the most common differential operators on manifolds is the covariant derivative [Pet06], which extends the notion of directional derivative for arbitrary manifolds. The covariant derivative $\nabla\omega$ of a 1-form ω returns a rank-2 tensor whose symmetric part is the Killing operator of ω, i.e., $\frac{1}{2}(\nabla\omega + \nabla\omega^t) := \mathcal{K}(\omega)$.[†] The Killing operator is, itself, remarkably relevant in differential geometry: its kernel corresponds to vector fields (known as

[†] Note that our definition of the Killing operator differs by a factor $1/2$ from most authors, in an effort to simplify further expressions.

Killing vector fields) that define isometric flows on the surface [BCBSG10]. For $P \equiv \mathcal{K}$ in Eq. (4), the adjoint operator P^* turns out to be the negated divergence operator div on tensors [BE69], implicitly defined on a closed surface as:

$$\langle \sigma, \mathcal{K}(\omega) \rangle_F = -\langle \operatorname{div} \sigma, \omega \rangle_1 \quad \forall \sigma \in \mathcal{S}. \tag{5}$$

Note that, for flat domains with the Euclidean metric I, the Killing operator can be expressed in local coordinates as a symmetric matrix with entry (i,j) of the form $\frac{1}{2}(\partial_j + \partial_i)$, while the divergence operator reduces to the divergence of each column of the matrix form of a tensor. From the Berger-Ebin decomposition, we conclude that any symmetric tensor field is composed of a divergence-free part plus an element of the image of the Killing operator:

$$\mathcal{S} = \operatorname{Im} \mathcal{K} \oplus \operatorname{Ker} \operatorname{div}. \tag{6}$$

Curl-based expression. We can also define a similar decomposition using this time the notion of curl of a tensor. In fact, the relationship between div and curl for 2-tensors in $\mathcal{M}$ is simple: just like the curl of a vector field is minus the divergence of its rotated version, for a 2-tensor σ we have $\operatorname{curl} \sigma := \operatorname{div}(\star \sigma \star^{-t})$, where $\star \sigma \star^{-t}$ is the $\star$-conjugate of σ. We thus get a Berger-Ebin decomposition

$$\mathcal{S} = \operatorname{Im} \overline{\mathcal{K}} \oplus \operatorname{Ker} \operatorname{curl}, \tag{7}$$

where the operator $\overline{\mathcal{K}}$ indicates the $\star$-conjugate of the Killing operator, i.e., $\overline{\mathcal{K}}(\omega) := \star \mathcal{K}(\omega) \star^{-t}$.

Trace-based expression. Another canonical operator on tensors is the trace tr. Its Berger-Ebin based decomposition is rather trivial since the adjoint of the trace is simply $\operatorname{tr}^*(z) = z\mathfrak{g}$ for any scalar function z, thus leading to:

$$\mathcal{S} = \operatorname{Im} \operatorname{tr}^* \oplus \operatorname{Ker} \operatorname{tr}. \tag{8}$$

2.4 Remarks

We conclude this section with a few observations.

Boundary conditions. In order to uniquely define the adjoint relation in Eq. (5), we must prescribe boundary conditions for 2-tensor fields. Similar to the case of 1-forms, this can be achieved by either prescribing boundary tensors (Dirichlet boundary condition) or specifying their normal derivatives (Neumann boundary condition).

Physical Interpretation. Tensor decompositions are often used to characterize deformations in mechanical systems. The antisymmetric part of asymmetric tensors (Eq. (2)), for instance, reveals infinitesimal rotations in a fluid motion. Divergence-free tensors and the Killing operator (Eq. (6)) indicate force equilibrium and deviation from isometries in solid mechanics. Similarly, the trace-based decomposition (Eq. (8)) identifies local dilations and shearing, commonly controlled in elasticity via Lamé parameters.

Covariant Derivative. As mentioned in §2.3, the covariant derivative maps a 1-form ω to a 2-tensor field $\nabla\omega$ which is the sum of a symmetric and an antisymmetric part:

$$\nabla \omega = \mathcal{K}(\omega) - \tfrac{1}{2} d\omega, \tag{9}$$

where the antisymmetric part is half the curl of the vector field $\omega^\sharp$ associated to ω. Therefore, the covariant derivative $\nabla\omega$ identifies the scalar function q in Eq. (3) with the (negated) function g induced by the coclosed part $\star dg$ of ω.

Generalized Laplacian. The standard Laplace-Beltrami operator Δ on a function z is defined as $\operatorname{div}(\nabla z)$. This operation generalizes for a symmetric 2-tensor field σ in $\mathcal{M}$ as

$$\Delta^\sigma z := \operatorname{div}(\sigma \nabla z) = \star(\operatorname{div} \sigma \wedge \star dz) + \operatorname{tr}\left(\sigma\, \mathfrak{g}^{-1} \operatorname{Hess}(z)\right), \tag{10}$$

where $\operatorname{Hess}(z)$ is the Hessian of z. This operator is particularly relevant in the computation of quasi-harmonic fields [AN02] and in elasticity [Hu54]. Graphics applications have also used this generalized Laplacian to compute anisotropic parameterization [ZRS05, KMZ11] and filtering [PM90], and more recently to design simplicial masonry structures [dGAOD13, LHS*13]. Note that, when σ is a divergence-free tensor field, the generalized Laplace operator becomes *linear accurate*, i.e., $\Delta^\sigma z = 0$ for any linear function z in the plane.

3 Tensor Fields over $2D$ Euclidean Space

We now combine the three Berger-Ebin decompositions described in §2.3, and derive a new coordinate-free decomposition of 2-tensor fields for the case of a compact region $\mathcal{M}$ in $\mathbb{R}^2$ with boundaries $\partial\mathcal{M}$ and Euclidean metric ($\mathfrak{g} \equiv I$). The continuous picture we present here will be at the core of our discrete approach to deal with 2-tensor fields on arbitrary triangulations. Notice that differential operators simplify considerably for the Euclidean case—e.g., the Hodge-star and the area form reduce to $\star \equiv J$ and $\mu_\mathfrak{g} \equiv J^t$, respectively. Yet we keep our original notation in order to discuss extensions and limitations of our results for curved surfaces.

Killing decomposition. Suppose that a 1-form ω is expressed, via Hodge decomposition, as $\omega = df \oplus \star dg \oplus h$, where f and g are scalar functions (df and $\star dg$ represent, respectively, the 1-forms associated to ∇f and $J\nabla g$), and h is a harmonic 1-form. Its Killing operator $\mathcal{K}(\omega)$ can be decomposed by linearity into terms that are mutually orthogonal with respect to the Frobenius inner product—not only in the plane, but also for surfaces of constant Gaussian curvature as shown in App. A:

$$\mathcal{K}(\omega) = \mathcal{K}(df) \oplus \mathcal{K}(\star dg) \oplus \mathcal{K}(h) = \operatorname{Hess}(f) \oplus \operatorname{Tr}^0(g) \oplus \nabla h. \tag{11}$$

One can check that $\mathcal{K}(df)$ reduces to the Hessian $\operatorname{Hess}(f) := \nabla df$ of the function f, while the term $\mathcal{K}(\star dg)$ is always traceless—we thus denote it as $\operatorname{Tr}^0(g)$. The term $\mathcal{K}(h)$ is simply the covariant derivative ∇h due to the harmonicity of h.

Conjugate Killing decomposition. In a similar fashion, the $\star$-conjugate version of the Killing operator $\overline{\mathcal{K}}(\omega)$ can, itself, be decomposed as:

$$\overline{\mathcal{K}}(\omega) = \star \operatorname{Hess}(f) \star^{-t} \oplus \star \operatorname{Tr}^0(g) \star^{-t} \oplus \star \nabla h \star^{-t}. \tag{12}$$

We note here that the traceless and harmonic terms in the plane are invariant by $\star$-conjugation; i.e., $\operatorname{Tr}^0(g) = \star \operatorname{Tr}^0(g) \star^{-t}$ and $\nabla h = \star \nabla h \star^{-t}$.

Complete decomposition. Using Eqs. (3), (11) and (12), and recalling that divergence-free tensors can be expressed as $\star$-conjugated Hessians [GZ02], we conclude that an arbitrary 2-tensor field τ in the plane is orthogonally decomposed into antisymmetric, divergence-free, curl-free, traceless, and harmonic parts:

$$\tau = \overbrace{s\mu_{\mathfrak{g}}}^{\in\mathcal{A}} \oplus \overbrace{\underbrace{\mathrm{Hess}(f)}_{\text{curl free}} \oplus \underbrace{\star\mathrm{Hess}(w)\star^{-t}}_{\text{div free}} \oplus \underbrace{\mathrm{Tr}^0(g)}_{\text{traceless}} \oplus \underbrace{\star\nabla h\star^{-t}}_{\text{harmonic}}}^{\in\mathcal{S}}, \quad (13)$$

where the scalar function s describes the antisymmetric part of the tensor field, and the three scalar functions (f, g and w) plus a harmonic 1-form h encode the space of symmetric tensors. Thereby, we obtain a *complete characterization of planar* 2*-tensor fields*, which only requires coordinate-free scalar functions f, g, w, and s.

We further notice that any constant tensor of the form $aI + bB + cC$ can be expressed as the Hessian of a quadratic function f or w. Similarly, a constant tensor $pJ + bB + cC$ can be associated to the covariant derivative of the rotated gradient of a quadratic function g. We can thus use the three constant scaling a, b, and c to encode a "mean" symmetric tensor field, and then rewrite Eq. (13) in a more concise form:

$$\tau = sJ + aI + bB + cC + \mathcal{K}(df + \star dg) + \overline{\mathcal{K}}(dw + h). \quad (14)$$

Separating these constant terms will be shown useful in our treatment of 2-tensors on discrete non-flat surfaces in §4.2.

Finally, it bears repeating that Eq. (13) is only valid for the Euclidean metric ($\mathfrak{g} \equiv I$). Moreover, while the Berger-Ebin decompositions presented in §2.3 are valid for any smooth manifold, we show in App. A that the various parts of the Killing operator in Eq. (11) are mutually orthogonal only on surfaces of constant Gaussian curvature. To our knowledge, there is no known general coordinate-free decomposition of 2-tensors on arbitrary surfaces.

4 Tensor Fields over Triangulations

We now leverage our continuous decomposition of 2-tensor fields in the plane to represent discrete 2-tensor fields on arbitrary triangle meshes via *local, discrete* 0- and 1*-forms*.

4.1 Discrete antisymmetric 2-tensors

Differential forms are known to be conveniently discretized using the concept of *cochains* defined in Algebraic Topology [Mun84], and can be interpolated through Whitney form bases [Whi57]. The resulting discrete differential forms [DKT08] and their most relevant operators [AFW06b] are well documented by now. In particular, Hodge decomposition of arbitrary forms carries very neatly into the discrete realm in a coordinate-free fashion. The case of discrete 2-forms is a particularly simple subset of this discrete theory: a 2-form μ as used in Eq. (3) is simply encoded as its integration over each face ijk

$$\mu_{ijk} = \int_{ijk} \mu. \quad (15)$$

This is equivalent to storing a scalar s_{ijk} per face as a discretization of the antisymmetric part in Eq. (14), with $s_{ijk} = \mu_{ijk}/a_{ijk}$. Note that this value can be further decomposed using the Laplacian of a dual 0-form q and a constant 2-form p as indicated in §2.1. From this set of scalar-per-face μ_{ijk}, a discrete differential 2-form can be interpolated through face-based Whitney basis functions as $\sum_{ijk} \mu_{ijk}\,\phi_{ijk}$.

4.2 Discrete symmetric 2-tensors

Unlike the antisymmetric case, symmetric tensors are not entities that are directly "integrable", thus a different discretization approach must be adopted. We introduce a finite-dimensional representation of symmetric tensors via a discrete version of Eq. (14).

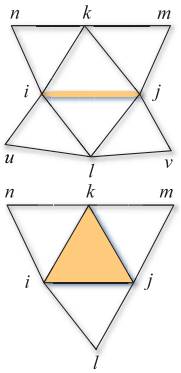

Encoding. We propose to represent discrete symmetric 2-tensor fields on arbitrary triangle meshes by encoding the forms involved in the decomposition of Eq. (14) over small, developable patches: we use *one patch per edge ij* defined as the "butterfly stencil" containing the two triangles adjacent to ij and their immediate neighbors, as well as *one patch per face ijk* defined as the face and its immediate flaps (see inset). For each edge-centered and face-centered patch, we store a local approximation of a continuous tensor field as values per oriented simplex (w_i and f_i at nodes, values g_{ijk} at triangles, and harmonic 1-form values h_{ij} at oriented edges) from which we will be able to derive the symmetric terms of Eq. (14). This form-based discretization choice is guided by the usual algebraic topology tools of DEC/FEEC and the resulting discrete Hodge decomposition [DKT08]: in particular, it faithfully discretizes the continuous 1-forms $df + \star dg$ and $dw + h$ as $\mathbf{d}_0 f + \bigstar^{-1}\mathbf{d}_1^t g$ and $\mathbf{d}_0 w + h$, where $\bigstar$ is a discrete Hodge star. Note that we do not need to explicitly encode the constants a, b, and c since, as we discussed in §3, they can be incorporated in the scalar fields f, g, w, and s.

Interpolation. As we wish to provide a discrete treatment of 2-tensors that is fully compatible with DEC, the use of Whitney form basis functions [Whi57] is most appropriate: they provide low order, intrinsic interpolation of our discrete forms through $f = \sum_i f_i \phi_i$, $g = \sum_i g_{ijk}\phi_{ijk}$, and $h = \sum_{ij} h_{ij}\phi_{ij}$. With this piecewise continuous reconstruction of forms over each patch, we can formally evaluate the local tensor field approximation for all patches as we describe below. However, our use of piecewise linear basis functions is not amenable to properly capture locally constant 2-tensors: while a quadratic function f has a constant Hessian, a piecewise-linear approximation of f fails to fulfill this property. We thus begin our tensor reconstruction by extracting a local mean tensor per patch, denoted $\overline{\sigma}$, to fully remedy this limitation of low-order form interpolation.

Extracting local mean tensor $\overline{\sigma}$. From f, g, w, h we first evaluate a local constant tensor $\overline{\sigma}$ through local fitting. For each of the 1-forms $\mathbf{d}_0 f$, $\star^{-1}\mathbf{d}_1^t g$, h, and $\mathbf{d}_0 w$ on an edge-based or face-based patch, we find the least-squares fitting linear 1-form over the patch: using a local coordinate system where x is along the oriented edge, we compute the optimal coefficients $\{\nu_i\}_{i=1..6}$ of the 1-form $\nu_1 dx+\nu_2 dy+\nu_3(xdx+ydy)+\nu_4(ydx+xdy)+\nu_5(xdx-ydy)+\nu_6(ydx-xdy)$. The mean tensor $\overline{\sigma}=aI+bB+cC$ is then expressed in local coordinates as a sum of contributions $\nu_3 I+\nu_4 B+\nu_5 C$ obtained from each 1-form $\mathbf{d}_0 f$, $\star^{-1}\mathbf{d}_1^t g$, h, and $\mathbf{d}_0 w$. This procedure requires a linear least-squares solve of size 6x6 for both edge- and face-based patches, and is performed on the fly when needed.

Residual edge-based Dirac tensors. The differential terms of Eq. (14), representing spatially varying terms around the mean tensor $\overline{\sigma}$, can now be captured within each patch as well. Once we remove from the values of $\mathbf{d}_0 f$, $\star^{-1}\mathbf{d}_1^t g$, $\mathbf{d}_0 w$, and h the linear 1-forms found in the least-squares solution, the residual discrete forms can be formally differentiated to find the corresponding tensor field they encode over each patch. Because of our choice of Whitney basis functions, the resulting residual 2-tensor field turns out to only include edge discontinuities induced by the derivatives of the piecewise linear bases ϕ_i and ϕ_{ij}. The Hessian of f, for instance, is trivially zero everywhere except *across* edges, since the vertex-based basis functions are piecewise linear inside each triangles, and their gradients are discontinuous across an edge. Similarly, the traceless term $\mathrm{Tr}^0(g)$ leads to discontinuities in the piecewise linear 1-form $\star^{-1}\mathbf{d}_1^t g$ across edges. In contrast, the $\star$-conjugate Hessian of w is zero everywhere except *along* edges. We can further compute the tensor term coming from the harmonic 1-form h as a discontinuity along every edge. (Note that the harmonic term could be locally absorbed in the function w due to Poincaré lemma, thereby reducing memory usage if needed; we keep it in our exposition for clarity.) Therefore, our discrete symmetric tensors boil down to a constant tensor $\overline{\sigma}$ plus a sum of impulse tensors on edges expressed as

$$\overline{\sigma}+\sum_{ij}\delta_{ij}\left[t_{ij}(\mathbf{d}_0 f+\star^{-1}\mathbf{d}_1^t g)\,\mathbf{e}_{ij}^{\perp}\otimes\mathbf{e}_{ij}^{\perp}+t_{ij}(\mathbf{d}_0 w+h)\mathbf{e}_{ij}\otimes\mathbf{e}_{ij}\right], \quad (16)$$

where $\mathbf{e}_{ij}$ is the normalized vector for edge ij, δ_{ij} is the line Dirac function along ij (i.e., $\delta_{ij}(x,y)=\delta(y)$ with δ being the 1D Dirac function and the x-axis being along ij), and t_{ij} is a function linear in its 1-form argument such that, for edge ij between triangles ijk and ilj, $t_{ij}=t_{ij}^k+t_{ji}^l$ with

$$\begin{aligned} t_{ij}^k(\alpha) &= \alpha_{ij}\left(\phi_j\cot\theta_{ijk}-\phi_i\cot\theta_{kij}\right)/l_{ij} \\ &\quad+\left(\alpha_{jk}\,\phi_j-\alpha_{ki}\,\phi_i\right)\left(\cot\theta_{kij}+\cot\theta_{ijk}\right)/l_{ij}. \end{aligned} \quad (17)$$

These impulse tensors are only well defined in a distributional sense, but they will be systematically integrated against basis functions in §5 to obtain weak forms of differential operators.

4.3 Discussion

Our proposed discrete encoding can be seen as a generalization of a number of previous approaches. First, our constant term $\overline{\sigma}$ per edge and per face is akin to the conventional piecewise-constant discretization of tensors, typically done per face or vertex—with the major difference that we do not need to define local frames in which components are stored: they are derived from our local, coordinate-free 0- and 1-forms instead. Second, edge-based Dirac tensors were already identified as relevant for triangulated surfaces (see, e.g., [CSM03, GGRZ06]); however, they were directly averaged per local neighborhood before being used for differential computations—instead, we keep the Dirac nature of our reconstructed tensors and formally integrate them to derive differential operators on scalars and vector fields. Lastly, having both constant tensors and Dirac edge tensors captures continuous tensor fields better than limiting the finite-dimensional representation to only one of these two parts.

We finally note that our representation is a generalization of the typical encoding of a stress tensor field in planar elastostatics via the Airy function [dGAOD13], which is the sum of a paraboloid and a function w—corresponding to a constant tensor field plus the rotated Hessian of w to represent a spatially-varying tensor field. This added non-constant term becomes a sum of Dirac impulses for linear basis functions; higher order Whitney elements (see, e.g., [AFW06b, WWT*06]) would remove Dirac distributions—at the cost of requiring larger patches.

5 Discrete Differential Tensor-based Operators

Our discrete 2-tensor edge-based representation can now be harnessed to define various operators on vector fields and/or 1-forms. For each tensor-based operator, we present its discrete expression for each of the terms in Eq. (14). We introduce the edge integration T_{ij}^k of the line Dirac function t_{ij}^k (Eq. (17)) as this term will appear in most expressions:

$$\begin{aligned} T_{ij}^k(\alpha) &= \int_{ijk}\delta_{ij}t_{ij}^k(\alpha) \\ &= \left(\alpha_{jk}\cot\theta_{kij}-\alpha_{ki}\cot\theta_{ijk}\right) \\ &\quad+\tfrac{1}{2}\left(\mathbf{d}_1\alpha\right)_{ijk}\left(\cot\theta_{ijk}-\cot\theta_{kij}\right), \end{aligned} \quad (18)$$

where α denotes a discrete 1-form. Following the convention for t_{ij}, we use $T_{ij}(\alpha):=T_{ij}^k(\alpha)+T_{ij}^l(\alpha)$. Observe that, in the case of exact 1-forms $\alpha=\mathbf{d}_0 f$, Eq. (18) simplifies to the non-conforming Laplacian [PP03] of f restricted to ijk. Consequently, the terms T_{ij} return zero for any linear function f. For a boundary edge ij, we set T_{ij} to zero in order to implement Neumann boundary condition.

5.1 Discrete generalized Laplacian $\nabla\cdot(\sigma\nabla)$

As mentioned in §2.4, the Laplacian operator of functions, commonly used in geometry processing, is a particular case of a general family of differential operators on functions $\Delta^\sigma(z)=\mathrm{div}\,(\sigma\nabla z)$ where σ is a symmetric 2-tensor field [AN02]. We can define its weak (integrated) form on

a discrete scalar function $z=\sum_j z_j\phi_j$ as

$$\langle\Delta^\sigma(z),\phi_i\rangle_0=\sum_{ij}(z_j-z_i)\int_M\sigma(\nabla\phi_i,\nabla\phi_j):=\sum_{ij}(z_i-z_j)\mathbf{H}^\sigma_{ij}. \quad (19)$$

This generalized Laplacian operator on discrete 0-forms can thus be expressed as a $|\mathcal{V}|\times|\mathcal{V}|$ matrix of the form

$$\Delta^\sigma=\mathbf{d}_0^t\mathbf{H}^\sigma\mathbf{d}_0, \quad (20)$$

where $\mathbf{H}^\sigma$ is a diagonal $|\mathcal{E}|\times|\mathcal{E}|$ matrix. Its coefficients $\mathbf{H}^\sigma_{ij}$ can be evaluated *in closed form* for the various types of σ presented in Eq. (14) as spelled out in App. C.

We point out that $\mathbf{H}^{\text{Id}}$ matches the diagonal Hodge star $\bigstar^{\text{D}}$ [BK99] traditionally used in mesh processing (we will discuss discrete Hodge star approximations further in §5.4). Also, the resulting elliptic operator Δ^{Id} reduces to the usual cotan-Laplacian operator [PP93]. Moreover, for the case of an exact 1-form $\omega=-\frac{1}{2}\mathbf{d}_0 w$, the matrix $\mathbf{H}^{\text{Hess}(w)}$ corresponds to the extra terms used in the *weighted Laplacian operator* [Gli05, MMdGD11]. Our formulation thus extends this operator to arbitrary 2-tensors, and due to our deliberate choice to use the conjugated form of the harmonic part in Eq. (13), our generalized Laplacian for $\omega=-\frac{1}{2}\mathbf{d}_0 w-h$ verifies the linear precision of its corresponding continuous operator [dGAOD13].

Ellipticity. In the continuous setting, the generalized Laplacian is (semi-)elliptic iff the symmetric 2-tensor σ is positive (semi-)definite (PSD). A full characterization of ellipticity of our resulting discrete generalized Laplacian is currently unknown, but many sufficient conditions can be (and have been) formulated. First, notice that a traceless 2-tensor cannot be PSD since the sum of its eigenvalues is zero. For the case $\sigma=\text{Hess}(w)$, a simple sufficient condition on the weights was offered in [Gli05], and it remains valid in our setup. For all other cases, one can directly check whether the discrete operator $\mathbf{H}^\sigma$ is positive definite by testing diagonal dominance and non-negativity.

5.2 Pairing through discrete tensors

Discrete symmetric tensors can also be used to pair with vector fields. The integral of this pairing, called total pairing, becomes an $|\mathcal{E}|\times|\mathcal{E}|$ operator on edge values since:

$$\langle\alpha,\sigma\beta^\sharp\rangle_1=\int_M\sigma(\alpha^\sharp,\beta^\sharp)=\sum_{ij,kl}\alpha_{ij}\beta_{kl}\int_M\sigma(\boldsymbol{\phi}_{ij},\boldsymbol{\phi}_{kl})=\alpha^t\mathbf{M}^\sigma\beta,$$

where α,β are discrete 1-forms corresponding to the vector fields $\alpha^\sharp,\beta^\sharp$. The matrix $\mathbf{M}^\sigma$ is typically referred to as the (generalized) *mass matrix*. App. D lists all the closed-form expressions of the pairing matrix $\mathbf{M}^\sigma$ for the terms of our decomposition in Eq. (14).

Inner products with symmetric tensors. A particularly important case of pairing through a symmetric 2-tensor σ is the notion of inner product, when σ is positive definite. As in the generalized Laplacian case, necessary and sufficient conditions on the scalar functions f and w to induce a positive definite matrix $\mathbf{M}^\sigma$ are not trivial to formulate. However, a simple check of the diagonal dominance and non-negativeness of $\mathbf{M}^{\mathcal{K}}$ and $\mathbf{M}^{\overline{\mathcal{K}}}$ provide a straightforward numerical characterization of inner products. Note that the mass matrix for $\sigma\equiv\text{Id}$ is the inner product of Whitney 1-form basis functions, dubbed the Galerkin Hodge star $\bigstar^{\text{G}}$ [BK99].

Cross products with antisymmetric tensors. We finally point out that when σ is purely antisymmetric (corresponding to the case $\sigma=\mu$ in Eq. (26)), the total pairing becomes an integrated cross product between the two vector fields weighted by the face values μ_{ijk}.

5.3 Trace

The discrete trace can also be defined through a weak form based on our discrete tensors, resulting in a value per vertex:

$$[\mathbf{tr}\,\sigma]_i=\langle\phi_i,\text{tr}(\sigma)\rangle_0.$$

Discrete antisymmetric tensors thus have zero discrete trace, as in the continuous world. For a discrete symmetric tensor σ equal to the sum in Eq. (16), and using $\int_{ijk}\phi_i\phi_j\mu_{\mathfrak{g}}=a_{ijk}/12$ and $\int_{ijk}\phi_i^2\mu_{\mathfrak{g}}=a_{ijk}/6$, we find:

$$[\mathbf{tr}\,\sigma]_i=\mathbf{d}_0^t\mathbf{H}^{\text{Id}}\mathbf{d}_0 w+\mathbf{d}_0^t\mathbf{M}^{\text{Id}}\omega.$$

The first term is the (primal) cotan-Laplacian of w at vertex i. The remainder is elucidated by noting that a discrete 1-form ω is naturally split based on the discrete Hodge decomposition induced by the Galerkin Hodge star ($\mathbf{M}^{\text{Id}}=\bigstar^{\text{G}}$ defined in Eq. (25)) as:

$$\omega=\mathbf{d}_0 f+\left(\mathbf{M}^{\text{Id}}\right)^{-1}\mathbf{d}_1^t g+h,$$

where h is closed and coclosed, i.e., $\mathbf{d}_1 h=0$ and $\mathbf{d}_0^t\mathbf{M}^{\text{Id}}h=0$. Since we know that $\mathbf{d}_0^t\mathbf{d}_1^t$ is null, the second term simplifies to the cotan-Laplacian of f, while the discrete versions of the traceless terms of the continuous decomposition (Eq. (13)) are zero with this discrete trace operator. Thus, the discrete trace recovers the exact same two non-zero terms as its continuous counterpart.

5.4 Choice of discrete Hodge stars

The continuous Hodge star can be approximated in the discrete setting in various ways. In our setup where discrete vector fields and 1-forms are expressed using edge values and Whitney basis functions, the most natural discrete Hodge star is arguably the Galerkin Hodge star $\bigstar^{\text{G}}\equiv\mathbf{M}^{\text{Id}}$ (Eq. (25)). However, the diagonal Hodge $\bigstar^{\text{D}}\equiv\mathbf{H}^{\text{Id}}$ (Eq. (23)) is a sparser alternative often preferred in graphics as it offers a less computationally intensive approximation—in particular, the discrete Hodge decomposition for this sparse star now only involves diagonal matrices. In fact, these two Hodge stars are well-known to be related in the sense that the primal Laplacian is the same whether Galerkin or diagonal approximation is used [BK99], i.e., $\mathbf{d}_0^t\bigstar^{\text{D}}\mathbf{d}_0=\mathbf{d}_0^t\bigstar^{\text{G}}\mathbf{d}_0$. Our extensions of $\bigstar^{\text{D}}$ and $\bigstar^{\text{G}}$ to arbitrary symmetric 2-tensors (resp., $\mathbf{H}^\sigma$ and $\mathbf{M}^\sigma$) precisely maintain this property as we prove in App. B. We thus note that one can opt for either one, but the use of the computationally-attractive diagonal approximation loses the traceless property of the terms in g and h described in §5.3 since $\mathbf{H}\mathbf{M}^{-1}$ no longer simplifies.

6 Applications

We now employ our discrete differential tensor-based operators to derive computational tools for covariant derivative, Lie bracket, and anisotropic geodesics on triangle meshes.

6.1 Discrete covariant derivative

The covariant derivative provides a generalization of directional derivatives on arbitrary surfaces. With this concept, one can measure the rate of change of a 1-form α along a vector field $\beta^\sharp$ (associated to a 1-form β) as the contraction of $\beta^\sharp$ with the 2-tensor $\nabla\alpha$:

$$\nabla_{\beta^\sharp}\alpha := (\nabla\alpha)\beta^\sharp = \omega,$$

where ω is the resulting 1-form. In the discrete realm, we make use of the piecewise linear basis function ϕ_{ij} to evaluate the directional derivative in a weak form as:

$$\forall ij,\ \langle \phi_{ij}, \omega\rangle_1 = \langle \phi_{ij}, (\nabla\alpha)\beta^\sharp\rangle_1.$$

By leveraging Eq. (9) and the mass matrices derived in §5.2, we convert this weak formulation into a sparse linear system:

$$\mathbf{M}^{\mathrm{Id}}\omega = \left(\mathbf{M}^{\mathcal{K}(\alpha)} - \tfrac{1}{2}\mathbf{M}^{\mathbf{d}_1\alpha}\right)\beta, \tag{21}$$

Therefore, we define the discrete covariant derivative of the 1-form α as the matrix:

$$\nabla\alpha = \left(\mathbf{M}^{\mathrm{Id}}\right)^{-1}\left(\mathbf{M}^{\mathcal{K}(\alpha)} - \tfrac{1}{2}\mathbf{M}^{\mathbf{d}_1\alpha}\right).$$

Note that the mass matrices are computed by combining the mean tensor $\overline{\sigma}$ extracted from α in each patch, the edge-based residual tensor defined by α, and the antisymmetric tensor $\mathbf{d}_1\alpha$. Matrix $\mathbf{M}^{\mathrm{Id}}$ is sparse, positive-definite, and depends only on the triangle mesh, it can thus be efficiently pre-factorized (our implementation uses `eigen` [GJ*10]). One can then compute directional derivatives for different 1-forms β through simple sparse matrix-vector multiplication and back substitution. Fig. 1 illustrates a directional derivative on a planar mesh with concave boundaries for the case $\alpha = -2xydx - x^2dy$ and $\beta = dx$. The resulting discrete 1-form ω provides an approximation of the analytical solution with a relative error of 0.7% for a coarse mesh and 0.1% for a 4x finer mesh. Fig. 2 exemplifies the robustness of the discrete covariant derivative to meshes with variable resolution (even in the presence of obtuse angles), while Fig. 3 shows directional derivatives on surfaces of complex shape and non-trivial topology. Finally, Fig. 7 presents convergence tests of our results with symmetric and asymmetric tensor fields; we restricted our analysis to a disk, a planar concave mesh and a sphere, since their directional derivatives have known analytical expressions. We also tested the contribution of the impulse tensors in Eq. (16) versus using simply the mean tensor $\overline{\sigma}$ per patch in our computations, and observed a systematic decrease in the relative residual from 2% to 27% depending on the tensor fields.

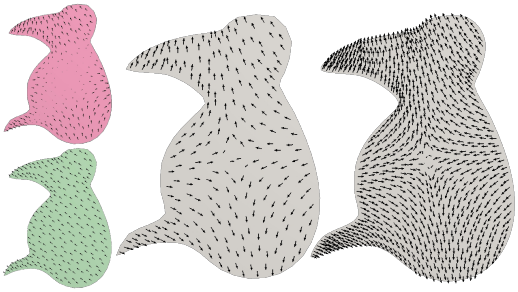

Figure 1: *Covariant derivative of a 1-form $\alpha = -2xydx - x^2dy$ (top-left) along $\beta = dx$ (bottom-left) for a planar mesh with concave boundary. Resulting 1-form ω has a numerical residual w.r.t. the analytical solution of 0.7% (center, $|\mathcal{V}| = 173$) and 0.1% (right, $|\mathcal{V}| = 609$), respectively. Vector fields are displayed by interpolating 1-forms at triangle barycenters.*

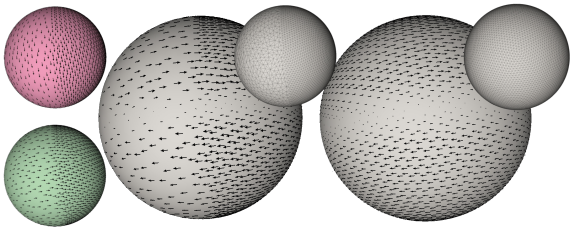

Figure 2: *For 1-forms $\alpha = \sin(\theta)d\theta$ (top left) and $\beta = \sin(\theta)d\phi$ (bottom left) (expressed in spherical coordinates), our discrete covariant derivative $\omega = \nabla_{\beta^\sharp}\alpha$ on an irregular mesh (center) is consistent with the result on a uniform mesh (right) (meshes shown as insets). Vector fields displayed by interpolating 1-forms at barycenters of a subset of triangles.*

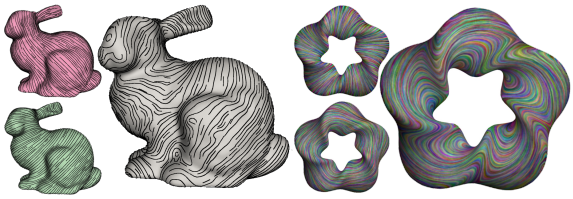

Figure 3: *Discrete covariant derivative on meshes of arbitrary shape and topology. We chose α (top) and β (bottom) as the smoothest 1-forms from the 1-form Laplacian [DKT08]. Central images show the resulting 1-form $\nabla_{\beta^\sharp}\alpha$, visualized with sampled integral curves (bunny) and line integral convolution [PZ11] (twisted torus).*

6.2 Discrete Lie bracket

Our discrete treatment of the covariant derivative also leads to a Lie bracket (also known as the commutator) of vector-fields. By flattening vector fields to 1-forms, the Lie bracket of two 1-forms α and β returns a 1-form γ evaluated as:

$$[\alpha, \beta] := \nabla_{\beta^\sharp}\alpha - \nabla_{\alpha^\sharp}\beta = \gamma.$$

From this definition, we directly reuse Eq. (21) and compute the discrete Lie bracket 1-form γ through a similar sparse linear system. Fig. 5 validates our discrete Lie bracket on the "torus example" proposed in [ABCCO13].

6.3 Anisotropic heat method

Discrete 2-tensors are also suitable to compute anisotropic geodesic distances based on a simple extension of the heat

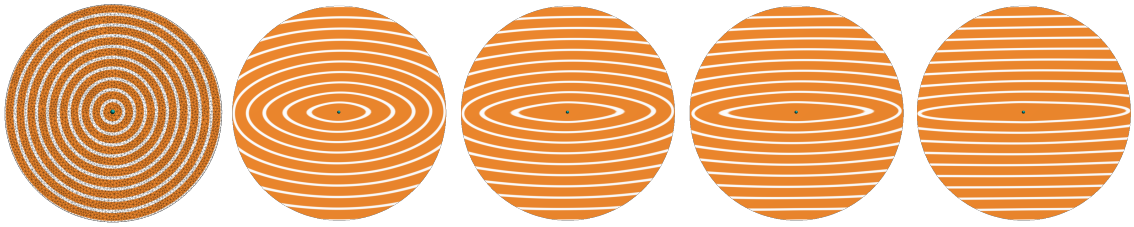

Figure 4: *Our tensor-based discrete differential operators can be used to compute anisotropic geodesics. We tested our method on a disk with constant tensors of various anisotropy ratio (from left to right:* 1, 0.5, 0.3, 0.2, *and* 0.1*), with the larger magnitude along the x-axis. Notice that the iso-levels stretch to ellipses with the anisotropy as expected.*

method [CWW13]. For geodesics induced by the Euclidean embedding space, the heat method requires two linear system solves involving the cotan-Laplace operator: the first step diffuses an impulse heat function z_0 isotropically for a short time interval ε into a function z, while the second step finds the potential ψ whose gradient best approximates the normalized gradient of z under the surface metric. We instead propose to replace the isotropic diffusion in the first step by an anisotropic diffusion [PM90] induced by a PSD symmetric 2-tensor field σ. We thus compute the function z using the generalized Laplacian operator $\mathbf{H}^{\sigma}$ (see §5.1):

$$\left(\bigstar_0 + \varepsilon\, \mathbf{d}_0^t \mathbf{H}^{\sigma} \mathbf{d}_0\right) z = \bigstar_0 z_0,$$

where $\bigstar_0$ is the diagonal Hodge-star for 0-forms using vertex areas [DKT08]. We further set the time step ε to the square of the averaged edge length measured with respect to the tensor σ. The second step remains unchanged, solving for the potential ψ based on the cotan-Laplacian matrix $\mathbf{d}_0^t \mathbf{H}^{\mathrm{Id}} \mathbf{d}_0$. For boundary conditions, we used Robin boundary conditions as advocated in [CWW13].

In Fig. 4, we demonstrate the accuracy of our method by illustrating isodistances for various anisotropy ratios on a unit disk mesh. We also compute anisotropic distances driven by curvature in Fig. 6: we first compute an average shape operator Λ per edge as in [CSM03], and set the mean tensor $\overline{\sigma}$ to $(I+0.1\Lambda^2)^{-1}$, such that distances evolve more slowly in regions of large curvature magnitudes.

7 Future Work

Our discrete symmetric 2-tensors and their associated operators on vector fields require further numerical analysis, just like usual operators in geometry processing [HPW06]. A higher order construction of symmetric tensors through the subdivision 1-form basis functions introduced in [WWT*06] would also be interesting (yet, more involved) so that the resulting discrete tensor fields could now be piecewise constant or linear. Moreover, our encoding of arbitrary 2-tensors may also find other applications in the context of simulation: the stress and strain tensors used in elasticity could be encoded with intrinsic values—instead of using a piecewise-constant representation induced by the embedding of the triangle mesh as typically done in finite-element methods. Encoding the second fundamental form on a triangle mesh could also be valuable. We are also investigating a discrete notion of Frobenius inner product consistent to our discrete 2-tensors, with which one can compute Killing vector fields [BCBSG10] and smoothness energies [KCPS13]. Finally, extending our discrete treatment of 2-tensors to tet meshes is another topic left for future work.

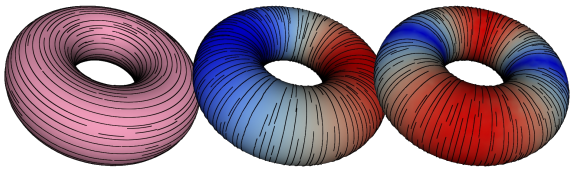

Figure 5: *Our discrete notion of Lie bracket reproduces the torus example presented in [ABCCO13] both qualitatively and quantitatively. For two* 1*-forms* α *(left) and* $z\beta$ *(middle), where* z *is a scaling function, the resulting Lie bracket* $\gamma = [\alpha, \beta]$ *(right) is parallel to* β*, as expected in the smooth case. Pseudo-colors indicate the norm of* $z\beta$ *and* γ*, respectively.*

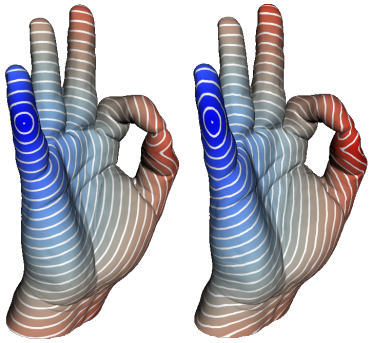

Figure 6: *Anisotropic geodesics can be computed guided by the curvature tensor of a surface. Left: isotropic geodesic distance generated by the heat method [CWW13]. Right: anisotropic (curvature-aware) geodesic distance computed with our generalized Laplacian operator (see §5.1).*

Acknowledgments. We thank Patrick Mullen for his feedback on a draft of this paper, and Dmitry Pavlov for early discussions. MD, MB, and FdG were partially supported through NSF grant CCF-1011944 and a PhD Google Fellowship, while YT and BL were partially supported through NSF grants IIS-0953096, CMMI-1250261 and III-1302285.

References

[AAW08] ARNOLD D. N., AWANOU G., WINTHER R.: Finite elements for symmetric tensors in three dimensions. *Math. Com-*

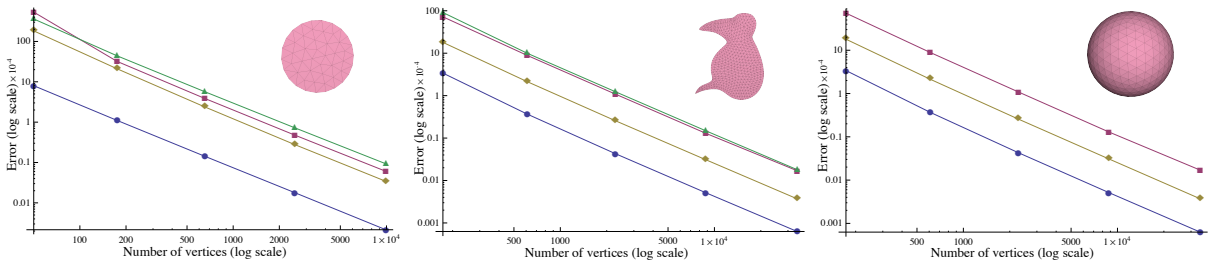

Figure 7: *Error plot in log-log scale of the residual of the discrete covariant derivative w.r.t. its analytical solution, indicating linear convergence on different meshes. For a disk mesh (left) and a concave shape (middle), we analyzed four scenarios: [in blue]* $\alpha = (x-y)dx+(x+y)dy$, $\beta = xdx+ydy$, $\nabla_{\beta^\sharp}\alpha = (x-y)dx+(x+y)dy$; *[in pink]* $\alpha = -2xydx-x^2dy$, $\beta = dx$, $\nabla_{\beta^\sharp}\alpha = -2(ydx+xdy)$; *[in yellow]* $\alpha = sin(2x)dx+cos(2y)dy$, $\beta = cos(2x)dx$, $\nabla_{\beta^\sharp}\alpha = 2cos(2x)^2dx$; *[in green]* $\alpha = x^2dx-2xydy$, $\beta = dx$, $\nabla_{\beta^\sharp}\alpha = 2(xdx-ydy)$. *For the sphere (right), we evaluated three cases which are, in spherical coordinates, [in blue]* $\alpha = sin(2\theta)d\theta$, $\beta = cos(2\theta)d\theta$, $\nabla_{\beta^\sharp}\alpha = 2cos^2(2\theta)d\theta$; *[in pink]* $\alpha = sin(2\theta)d\phi$, $\beta = cos(2\theta)d\theta$, $\nabla_{\beta^\sharp}\alpha = 2cos^2(2\theta)d\phi$; *[in yellow]* $\alpha = sin(2\theta)d\theta+sin(2\theta)d\phi$, $\beta = cos(2\theta)d\theta$, $\nabla_{\beta^\sharp}\alpha = 2cos^2(2\theta)d\theta+2cos^2(2\theta)d\phi$. *Errors measured using only the mean tensor* $\overline{\sigma}$ *(with no edge-based residual tensors) can be up to 27% larger.*

put. 77 (2008), 1229–1251. 2

[AAW14] ARNOLD D. N., AWANOU G., WINTHER R.: Nonconforming tetrahedral mixed finite elements for elasticity. *Math. Models Methods Appl. Sci. 24* (2014), 783–796. 2

[ABCCO13] AZENCOT O., BEN-CHEN M., CHAZAL F., OVSJANIKOV M.: An operator approach to tangent vector field processing. *Comp. Graph. Forum 32*, 5 (2013), 73–82. 1, 8, 9

[ACSD*03] ALLIEZ P., COHEN-STEINER D., DEVILLERS O., LÉVY B., DESBRUN M.: Anisotropic polygonal remeshing. *ACM Trans. Graph. 22*, 3 (2003). 2

[AFW06a] ARNOLD D. N., FALK R. S., WINTHER R.: Differential complexes and stability of finite element methods II: The elasticity complex. In *Compatible Spatial Discretizations*, Arnold D., Bochev P., Lehoucq R., Nicolaides R., Shashkov M., (Eds.), vol. 142 of *IMA Vol. Math. Appl.* 2006, pp. 47–68. 2

[AFW06b] ARNOLD D. N., FALK R. S., WINTHER R.: Finite element exterior calculus, homological techniques, and applications. *Acta Numerica 15* (2006), 1–155. 2, 5, 6

[AMR88] ABRAHAM R., MARSDEN J., RATIU R.: *Manifolds, Tensor Analysis, and Applications*. Springer, 1988. 2, 3

[AN02] ALESSANDRINI G., NESI V.: Area formulas for σ-harmonic mappings. In *Nonlinear Problems in Mathematical Physics and Related Topics I*, vol. 1 of *International Mathematical Series*. Springer US, 2002, pp. 1–21. 2, 4, 6

[AW02] ARNOLD D. N., WINTHER R.: Mixed finite elements for elasticity. *Numer. Math. 92*, 3 (2002), 401–419. 2

[AW03] ARNOLD D. N., WINTHER R.: Nonconforming mixed elements for elasticity. *Math. Models Methods Appl. Sci. 13*, 3 (2003), 295–307. 2

[BCBSG10] BEN-CHEN M., BUTSCHER A., SOLOMON J., GUIBAS L.: On discrete Killing vector fields & patterns on surfaces. *Comp. Graph. Forum 29*, 5 (2010), 1701–1711. 2, 4, 9, 11

[BE69] BERGER M., EBIN D. G.: Some decompositions of the space of symmetric tensors on a Riemannian manifold. *J. Differential Geom. 3-4* (1969), 379–392. 3, 4

[BH06] BOCHEV P. B., HYMAN J. M.: Principles of Mimetic Discretizations of Differential Operators. *IMA Volumes 142* (2006), 89–119. 2

[BK99] BOSSAVIT A., KETTUNEN L.: Yee schemes on a tetrahedral mesh, with diagonal lumping. *Int. J. Num. Model. 12* (1999), 129–142. 7, 12

[CHK13] CAMPEN M., HEISTERMANN M., KOBBELT L.: Practical anisotropic geodesy. *Comp. Graph. Forum 32*, 5 (2013), 63–71. 2

[CSM03] COHEN-STEINER D., MORVAN J.-M.: Restricted Delaunay triangulations and normal cycle. In *Symp. Comp. Geo.* (2003), pp. 312–321. 6, 9

[CWW13] CRANE K., WEISCHEDEL C., WARDETZKY M.: Geodesics in heat: A new approach to computing distance based on heat flow. *ACM Trans. Graph. 32*, 5 (2013). 2, 9

[dGAOD13] DE GOES F., ALLIEZ P., OWHADI H., DESBRUN M.: On the equilibrium of simplicial masonry structures. *ACM Trans. Graph. 32*, 4 (2013). 2, 4, 6, 7

[dGMMD14] DE GOES F., MEMARI P., MULLEN P., DESBRUN M.: Weighted triangulations for geometry processing. *ACM Trans. Graph. 33* (2014). 2

[DH94] DELMARCELLE T., HESSELINK L.: The topology of symmetric, second-order tensor fields. In *IEEE Visualization* (1994), pp. 140–147. 2

[DKT08] DESBRUN M., KANSO E., TONG Y.: Discrete differential forms for computational modeling. In *Discrete Differential Geometry,* A. I. Bobenko *et al.* (Eds), vol. 38 of *Oberwolfach Seminars*. Birkhäuser Basel, 2008, pp. 287–324. 2, 3, 5, 8, 9

[ETK*07] ELCOTT S., TONG Y., KANSO E., SCHRÖDER P., DESBRUN M.: Stable, circulation-preserving, simplicial fluids. *ACM Trans. Graph. 26*, 1 (2007). 2

[FH96] FRANK J. B., HECKBERT P. S.: A pliant method for anisotropic mesh generation. In *International Meshing Roundtable* (1996), pp. 63–76. 2

[FSDH07] FISHER M., SCHRÖDER P., DESBRUN M., HOPPE H.: Design of tangent vector fields. *ACM Trans. Graph. 26*, 3 (2007). 1

[GGRZ06] GRINSPUN E., GINGOLD Y. I., REISMAN J., ZORIN D.: Computing discrete shape operators on general meshes. *Comput. Graph. Forum 25*, 3 (2006), 547–556. 6

[GJ*10] GUENNEBAUD G., JACOB B., ET AL.: Eigen v3. http://eigen.tuxfamily.org, 2010. 8

[Gli05] GLICKENSTEIN D.: Geometric triangulations & discrete Laplacians on manifolds, 2005. arXiv.org:math/0508188. 7

[GZ02] GREEN A., ZERNA W.: *Theoretical Elasticity*. Dover, 2002. 5

[HPW06] HILDEBRANDT K., POLTHIER K., WARDETZKY M.: On convergence of metric and geometric properties of polyhedral surfaces. *Geometriae Dedicata 123*, 1 (2006), 89–112. 9

[Hu54] HU H. C.: Some variational principles in elasticity and plasticity. *Acta Phys. Sin. 10*, 3 (1954), 259–290. 2, 4

[IO06] IBEN H. N., O'BRIEN J. F.: Generating surface crack patterns. In *Symp. Comp. Anim.* (2006), pp. 177–185. 2

[KASH13] KRATZ A., AUER C., STOMMEL M., HOTZ I.: Visualization and analysis of second-order tensors: Moving beyond the symmetric positive-definite case. *Comp. Graph. Forum 32*, 1 (2013), 49–74. 2

[KAT*07] KANSO E., ARROYO M., TONG Y., YAVARI A., MARSDEN J., DESBRUN M.: On the geometric character of stress. *ZAMP 58(5)* (2007), 843–856. 2

[KCPS13] KNÖPPEL F., CRANE K., PINKALL U., SCHRÖDER P.: Globally optimal direction fields. *ACM Trans. Graph. 32*, 4 (2013). 1, 9

[KMZ11] KOVACS D., MYLES A., ZORIN D.: Anisotropic quadrangulation. *Computer Aided Geometric Design 28*, 8 (2011), 449–462. 2, 4

[LHS*13] LIU Y., HAO P., SNYDER J., WANG W., GUO B.: Computing self-supporting surfaces by regular triangulation. *ACM Trans. Graph. (SIGGRAPH) 32*, 4 (2013). 4

[Luo10] LUO F.: Rigidity of polyhedral surfaces, III, 2010. arXiv:1010.3284v1. 2

[LW09] LAIDLAW D., WEICKERT J.: *Visualization and Processing of Tensor Fields: Advances and Perspectives*, 1st ed. Springer Publishing Company, Incorporated, 2009. 2

[Mei03] MEIER D. L.: Constrained transport algorithms for numerical relativity. i. development of a finite-difference scheme. *The Astrophysical Journal 595* (2003), 980–991. 2

[MMdGD11] MULLEN P., MEMARI P., DE GOES F., DESBRUN M.: HOT: Hodge-optimized triangulations. *ACM Trans. Graph. (SIGGRAPH) 30* (2011). 7

[Mun84] MUNKRES J. R.: *Elements of Algebraic Topology*. Addison-Wesley, 1984. 5

[NSO12] NARAIN R., SAMII A., O'BRIEN J. F.: Adaptive anisotropic remeshing for cloth simulation. *ACM Trans. Graph. 31*, 6 (2012). 2

[Pet06] PETERSEN P.: *Riemannian Geometry*, vol. 171 of *Graduate Texts in Mathematics*. Springer, 2006. 3, 11

[PLC*11] PALKE D., LIN Z., CHEN G., YEH H., VINCENT P., LARAMEE R., ZHANG E.: Asymmetric tensor field visualization for surfaces. *IEEE Trans. Vis. Comp. Graph. 17*, 12 (2011), 1979–1988. 2

[PM90] PERONA P., MALIK J.: Scale-space and edge detection using anisotropic diffusion. *IEEE Trans. Pattern Anal. Mach. Intell. 12*, 7 (1990), 629–639. 4, 9

[PMT*11] PAVLOV D., MULLEN P., TONG Y., KANSO E., MARSDEN J., DESBRUN M.: Structure preserving discretization of incompressible fluids. *Physica D 240(6)* (2011), 443–458. 1

[PP93] PINKALL U., POLTHIER K.: Computing discrete minimal surfaces & their conjugates. *Exp. Math. 2*, 1 (1993), 15–36. 7, 12

[PP00] POLTHIER K., PREUSS E.: Variational approach to vector field decomposition. In *EG Data Vis.* 2000, pp. 147–155. 1

[PP03] POLTHIER K., PREUSS E.: Identifying vector field singularities using a discrete hodge decomposition. In *Vis. & Math.*, Hege, Polthier, (Eds.). Springer Verlag, 2003, pp. 113–134. 1, 6

[PPTSH14] PANOZZO D., PUPPO E., TARINI M., SORKINE-HORNUNG O.: Frame fields: Anisotropic and non-orthogonal cross fields. *ACM Trans. Graph. (SIGGRAPH) 33*, 4 (2014). 2

[PZ11] PALACIOS J., ZHANG E.: Interactive visualization of rotational symmetry fields on surfaces. *IEEE Trans. Vis. Comp. Graph. 17*, 7 (2011), 947–955. 8

[Reg61] REGGE T.: General relativity without coordinates. *Nuovo Cim. 19*, 3 (1961), 558–571. 2

[SSP08] SPRINGBORN B., SCHRÖDER P., PINKALL U.: Conformal equivalence of triangle meshes. *ACM Trans. Graph. 27*, 3 (2008). 2

[TLHD03] TONG Y., LOMBEYDA S., HIRANI A. N., DESBRUN M.: Discrete multiscale vector field decomposition. *ACM Trans. Graph. 22*, 3 (2003), 445–452. 1

[TSS*04] TEWARI G., SNYDER J., SANDER P. V., GORTLER S. J., HOPPE H.: Signal-specialized parameterization for piecewise linear reconstruction. In *Symp. Geom. Proc.* (2004), pp. 55–64. 2

[Whi57] WHITNEY H.: *Geometric Integration Theory*. Princeton University Press, 1957. 1, 3, 5

[WWT*06] WANG K., WEIWEI, TONG Y., DESBRUN M., SCHRÖDER P.: Edge subdivision schemes and the construction of smooth vector fields. *ACM Trans. Graph. 25*, 3 (2006), 1041–1048. 6, 9

[ZMT06] ZHANG E., MISCHAIKOW K., TURK G.: Vector field design on surfaces. *ACM Trans. Graph. 25*, 4 (2006), 1294–1326. 1

[ZP05] ZHENG X., PANG A.: 2D asymmetric tensor analysis. In *IEEE Visualization* (2005), pp. 3–10. 2

[ZRS05] ZAYER R., ROSSL C., SEIDEL H.-P.: Discrete tensorial quasi-harmonic maps. In *Shape Model. Int.* (2005), pp. 278–287. 2, 4

[ZYLL09] ZHANG E., YEH H., LIN Z., LARAMEE R.: Asymmetric tensor analysis for flow visualization. *IEEE Trans. Vis. Comp. Graph. 15*, 1 (2009), 106–122. 2

A Decomposition of Killing operator

We now detail the decomposition of the Killing operator $\mathcal{K}$ for smooth surfaces with Gaussian curvature κ. We first make use of the Bochner technique (see, e.g., [Pet06, BCBSG10]), and expand the divergence of the Killing operator as:

$$-\operatorname{div}(\mathcal{K}(\omega)) = (2d\delta + \delta d - 2\kappa I)\,\omega, \tag{22}$$

where $\delta := -\star d \star$ is a shorthand for the co-differential operator. (Note that we assumed a 1-form ω with zero Dirichlet or Neumann boundary condition for simplicity.) By combining Eqs. (5) and (22), we now compute the inner product of symmetric 2-tensor fields generated by the Killing operator of exact 1-forms df, co-exact 1-forms $\star dg$, and harmonic 1-forms h:

$$\begin{cases} \langle \mathcal{K}(df), \mathcal{K}(\star dg)\rangle_F = 2\langle f, \star(d\kappa \wedge dg)\rangle_0, \\ \langle \mathcal{K}(df), \mathcal{K}(h)\rangle_F = 2\langle f, \star(d\kappa \wedge \star h)\rangle_0, \\ \langle \mathcal{K}(\star dg), \mathcal{K}(h)\rangle_F = 2\langle g, \star(d\kappa \wedge h)\rangle_0. \end{cases}$$

These expressions return zero for arbitrary f, g and h *iff* the Gaussian curvature κ is constant. Therefore, we can decompose the Killing operator $\mathcal{K}$ into an orthogonal direct sum as stated in Eq. (11) in that case.

B Lumping of pairing

The proof found in [BK99] that the diagonal Hodge star is a lumping of the Galerkin Hodge star in the Laplacian operator extends directly to our discrete pairing operators for arbitrary symmetric tensors since:

$$\begin{aligned}\left(\mathbf{d}_0^t M^\sigma \mathbf{d}_0\right)_{ij} &= \sum_{kl,mn} \left(\mathbf{d}_0^t\right)^{kl,i} \left(\int_M \sigma(\boldsymbol{\phi}_{kl},\boldsymbol{\phi}_{mn})\right) \mathbf{d}_0^{mn,j} \\ &= \int_M \sigma\left(\sum_{kl} \mathbf{d}_0^{kl,i}\boldsymbol{\phi}_{kl}, \sum_{mn} \mathbf{d}_0^{mn,j}\boldsymbol{\phi}_{mn}\right) \\ &= \int_M \sigma(\nabla\phi_i,\nabla\phi_j) = \left(\mathbf{d}_0^t H^\sigma \mathbf{d}_0\right)_{ij}.\end{aligned}$$

C Discrete generalized Laplacian Δ^σ

The matrix $\mathbf{H}^\sigma$ is provided in closed form for the various terms of the decomposition in Eq. (14). Note that the evaluation stencil for each element requires the "butterfly" patch of edge ij (or part thereof), and we use the naming convention described in the inset of §4.2.

• **Case** $\sigma = I$**.** This case corresponds to the well-known cotan formula [PP93]:

$$\mathbf{H}^{\mathrm{Id}}_{ij} = \tfrac{1}{2}\left(\cot\theta_{jki} + \cot\theta_{ilj}\right) \tag{23}$$

• **Case** $\sigma = \mu$**.**

$$\mathbf{H}^{\mu}_{ij} = \tfrac{1}{2a_{jil}}\mu_{jil} - \tfrac{1}{2a_{ijk}}\mu_{ijk}. \tag{24}$$

• **Case** $\sigma = \mathcal{K}(\mathbf{d}_0 f + \bigstar^{-1}\mathbf{d}_1^t g)$**.** Using $\omega \equiv \mathbf{d}_0 f + \bigstar^{-1}\mathbf{d}_1^t g$ for conciseness, we have:

$$\begin{aligned}\mathbf{H}^{\mathcal{K}}_{ij} = &-\tfrac{1}{2l_{ij}^2}\left(\cot\theta_{kij}\cot\theta_{ijk} + \cot\theta_{jil}\cot\theta_{lji}\right) T_{ij}(\omega) \\ &+\tfrac{1}{4a_{ijk}}\cot\theta_{jki}\left(T_{ik}(\omega) + T_{kj}(\omega)\right) \\ &+\tfrac{1}{4a_{jil}}\cot\theta_{ilj}\left(T_{li}(\omega) + T_{jl}(\omega)\right)\end{aligned}$$

• **Case** $\sigma = \overline{\mathcal{K}}(\mathbf{d}_0 w + h)$**.**

$$\mathbf{H}^{\overline{\mathcal{K}}}_{ij} = \tfrac{1}{l_{ij}^2} T_{ij}(\mathbf{d}_0 w + h)$$

• **Case** $\sigma = B$**.**

$$\mathbf{H}^{B}_{ij} = \frac{cot\theta_{kij} - cot\theta_{ijk}}{2(cot\theta_{kij} + cot\theta_{ijk})} + \frac{cot\theta_{lji} - cot\theta_{jik}}{2(cot\theta_{jil} + cot\theta_{lji})}$$

• **Case** $\sigma = C$**.**

$$\mathbf{H}^{C}_{ij} = -\frac{1 + cot\theta_{kij}cot\theta_{ijk}}{2(cot\theta_{kij} + cot\theta_{ijk})} - \frac{1 + cot\theta_{jik}cot\theta_{lji}}{2(cot\theta_{jil} + cot\theta_{lji})}$$

D Pairing through discrete tensors

The matrix $\mathbf{M}^\sigma$ is provided in closed form for the various terms of the decomposition in Eq. (14). Note that the evaluation stencil for each element requires *either* the "butterfly" patch of edge ij *or* the patch of a face ijk, and we still use the naming convention described in the inset of §4.2.

• **Case** $\sigma = I$**.**

$$\begin{aligned}\mathbf{M}^{\mathrm{Id}}_{ij,ij} &= \tfrac{1}{4}\left(\cot\theta_{jki} + \cot\theta_{ilj}\right) \\ &\quad + \tfrac{1}{12}\left(\cot\theta_{kij} + \theta_{ijk}\right) + \tfrac{1}{12}\left(\cot\theta_{jil} + \cot\theta_{lji}\right) \\ \mathbf{M}^{\mathrm{Id}}_{ij,jk} &= \tfrac{1}{12}\left(\cot\theta_{ijk} - \cot\theta_{kij} - \cot\theta_{jki}\right).\end{aligned} \tag{25}$$

This resulting matrix $\mathbf{M}^{\mathrm{Id}}$ corresponds to the Galerkin Hodge star $\bigstar^G$ [BK99], as further discussed in §5.4.

• **Case** $\sigma = \mu$**.**

$$\mathbf{M}^{\mu}_{ij,jk} = -\mathbf{M}^{\mu}_{jk,ij} = -\frac{\mu_{ijk}}{6a_{ijk}}, \quad \mathbf{M}^{\mu}_{ij,ij} = 0. \tag{26}$$

• **Case** $\sigma = B$**.** We need to define a local coordinate frame to compute this pairing. For diagonal terms $\mathbf{M}^B_{ij,ij}$, we use the coordinate frame induced by the edge ij of the butterfly patch; for the other terms $\mathbf{M}^B_{ij,jk}$, we pick a random, but fixed frame F_{ijk} per face, and denote by η the angle that rotates the x direction of the local frame F_{ijk} to the direction of edge ki. With this convention, one gets:

$$\begin{aligned}\mathbf{M}^{B}_{ij,ij} &= \frac{cot\theta_{ijk} - cot\theta_{kij}}{4(cot\theta_{ijk} + cot\theta_{kij})} + \frac{cot\theta_{jil} - cot\theta_{lji}}{4(cot\theta_{jil} + cot\theta_{lji})} \\ \mathbf{M}^{B}_{ij,jk} &= sin(2\eta)\frac{1 + cot\theta_{jki}cot\theta_{kij} + (cot\theta_{jki} + cot\theta_{kij})^2}{12(cot\theta_{jki} + cot\theta_{kij})} \\ &\quad + cos(2\eta)\frac{cot\theta_{kij} - cot\theta_{jki}}{12(cot\theta_{jki} + cot\theta_{kij})}\end{aligned}$$

• **Case** $\sigma = C$**.** Using the same convention as above:

$$\begin{aligned}\mathbf{M}^{C}_{ij,ij} &= \frac{3 + cot\theta_{ijk}cot\theta_{kij} - cot^2\theta_{ijk} - cot^2\theta_{kij}}{12(cot\theta_{ijk} + cot\theta_{kij})} \\ &\quad + \frac{3 + cot\theta_{lji}cot\theta_{jil} - cot^2\theta_{lji} - cot^2\theta_{jil}}{12(cot\theta_{jil} + cot\theta_{lji})} \\ \mathbf{M}^{C}_{ij,jk} &= cos(2\eta)\frac{1 + cot\theta_{jki}cot\theta_{kij} + (cot\theta_{jki} + cot\theta_{kij})^2}{12(cot\theta_{jki} + cot\theta_{kij})} \\ &\quad - sin(2\eta)\frac{cot\theta_{kij} - cot\theta_{jki}}{12(cot\theta_{jki} + cot\theta_{kij})}\end{aligned}$$

• **Case** $\sigma = \mathcal{K}(\mathbf{d}_0 f + \bigstar^{-1}\mathbf{d}_1^t g)$**.** Using $\omega \equiv \mathbf{d}_0 f + \bigstar^{-1}\mathbf{d}_1^t g$ for conciseness, the closed form expression is:

$$\begin{aligned}\mathbf{M}^{\mathcal{K}}_{ij,jk} = \tfrac{1}{24a_{ijk}}\Big[&T_{ij}(\omega)\left(2\cot\theta_{ijk} - \cot\theta_{kij}\right) \\ &+ T_{jk}(\omega)\left(2\cot\theta_{ijk} - \cot\theta_{jki}\right) \\ &- T_{ki}(\omega)\left(\cot\theta_{jki} + \cot\theta_{kij}\right) \\ &+ \tfrac{1}{2}\cot\theta_{ijk}\left(\cot\theta_{kij} - \cot\theta_{jki}\right)(\mathbf{d}_1\omega)_{ijk} \\ &- \tfrac{1}{2}\cot\theta_{ijk}\left(\cot\theta_{jil} + \cot\theta_{lji}\right)(\mathbf{d}_1\omega)_{jil} \\ &+ \tfrac{1}{2}\cot\theta_{ijk}\left(\cot\theta_{kjm} + \cot\theta_{mkj}\right)(\mathbf{d}_1\omega)_{kjm}\Big]\end{aligned}$$

$$\begin{aligned}\mathbf{M}^{\mathcal{K}}_{ij,ij} = \tfrac{T_{ij}(\omega)}{6l_{ij}^2}\Big[&\cot^2\theta_{kij} + \cot^2\theta_{ijk} - \cot\theta_{kij}\cot\theta_{ijk} \\ &+ \cot^2\theta_{jil} + \cot^2\theta_{lji} - \cot\theta_{jil}\cot\theta_{lji}\Big] \\ + \tfrac{1}{12a_{ijk}}\Big[&T_{jk}(\omega)\left(\cot\theta_{ijk} + \cot\theta_{jki}\right) \\ &+ T_{ki}(\omega)\left(\cot\theta_{jki} + \cot\theta_{kij}\right)\Big] \\ + \tfrac{1}{12a_{jil}}\Big[&T_{il}(\omega)\left(\cot\theta_{jil} + \cot\theta_{ilj}\right) \\ &+ T_{lj}(\omega)\left(\cot\theta_{ilj} + \cot\theta_{lji}\right)\Big] \\ + \tfrac{(\mathbf{d}_1\omega)_{ijk}}{48a_{ijk}}\Big[&2\cot\theta_{jki}\left(\cot\theta_{kij} - \cot\theta_{ijk}\right) + \cot^2\theta_{lji} - \cot^2\theta_{jil}\Big] \\ + \tfrac{1}{48a_{ijk}}\Big[&(\mathbf{d}_1\omega)_{kjm}\left(\cot\theta_{kjm} + \cot\theta_{mkj}\right)\left(\cot\theta_{ijk} + \cot\theta_{jki}\right) \\ &- (\mathbf{d}_1\omega)_{ikn}\left(\cot\theta_{nik} + \cot\theta_{ikn}\right)\left(\cot\theta_{kij} + \cot\theta_{jki}\right)\Big] \\ + \tfrac{(\mathbf{d}_1\omega)_{jil}}{48a_{jil}}\Big[&2\cot\theta_{ilj}\left(\cot\theta_{lji} - \cot\theta_{jil}\right) + \cot^2\theta_{kij} - \cot^2\theta_{ijk}\Big] \\ + \tfrac{1}{48a_{jil}}\Big[&(\mathbf{d}_1\omega)_{liu}\left(\cot\theta_{liu} + \cot\theta_{uil}\right)\left(\cot\theta_{ilj} + \cot\theta_{jil}\right) \\ &- (\mathbf{d}_1\omega)_{jlv}\left(\cot\theta_{vjl} + \cot\theta_{jlv}\right)\left(\cot\theta_{ilj} + \cot\theta_{lji}\right)\Big]\end{aligned}$$

• **Case** $\sigma = \overline{\mathcal{K}}(\mathbf{d}_0 w + h)$**.**

$$\mathbf{M}^{\overline{\mathcal{K}}}_{ij,jk} = 0, \qquad \mathbf{M}^{\overline{\mathcal{K}}}_{ij,ij} = -\frac{1}{l_{ij}^2} T_{ij}(\mathbf{d}_0 w + h)$$

The similarity of this last diagonal term with $\mathbf{H}^{\overline{\mathcal{K}}}$ is explained in §5.4 where Hodge star approximations are discussed.